Efficient Mobile Fronthaul via DSP-Based Channel Aggregation

Xiang Liu, *Senior Member, IEEE, Fellow, OSA*, Huaiyu Zeng, *Member, IEEE*, Naresh Chand, *Fellow, IEEE*, and Frank Effenberger, *Fellow, IEEE, Fellow, OSA*

(Invited Paper)

***Abstract*—Mobile fronthaul is an important network segment that bridges wireless baseband units and remote radio units to support cloud radio access network. We review recent progresses on the use of frequency-division multiplexing to achieve highly bandwidth-efficient mobile fronthaul with low latency. We present digital signal processing (DSP) techniques for channel aggregation and deaggregation, frequency-domain windowing, adjacent channel leak age ratio reduction, and synchronous transmission of both the I/Q waveforms of wireless signals and the control words (CWs) used for control and management purposes. In a proof-of-concept experiment, we demonstrate the transmission of 48 20-MHz LTE signals with a common public radio interface (CPRI) equivalent data rate of 59 Gb/s, achieving a low round-trip DSP latency of <2 μs and a low mean error-vector magnitude (EVM) of $\sim$2.5% after fiber transmission. In a follow-up experiment, we further demonstrate the transmission of 32 20-MHz LTE signals together with CPRI-compliant CWs, corresponding to a CPRI-equivalent data rate of 39.32 Gb/s, in single optical wavelength channel that requires an RF bandwidth of only $\sim$1.6 GHz. After transmission over 5-km standard single-mode fiber, the CWs are recovered without error, while the LTE signals are recovered with an EVM of lower than 3%. Applying this technique to future 5G wireless networks with massive multiple-input multiple-output is also discussed. This efficient mobile fronthaul technique may find promising applications in future integrated fiber/wireless access networks to provide ultrabroadband access services.**

***Index Terms*—Cloud radio access network (C-RAN), common public radio interface (CPRI), fifth-generation (5G), frequency-division multiplexing (FDM), mobile fronthaul, optical fiber transmission.**

I. Introduction

CLOUD optical radio access network (C-RAN) is expected to play important role in future mobile networks [1]–[6]. C-RAN improves network performance via coordinated multi-point (CoMP) and increases network energy efficiency via capacity sharing and optimization. It also effectively enables massive multiple-input-multiple-output (M-MIMO), which is considered as a key technology for the fifth-generation (5G) mobile networks [7]. Mobile fronthaul is a key network element in the C-RAN architecture, as it connects centralized baseband units (BBUs) with remote radio units. The interface used for mobile fronthaul is primarily based on the common public radio interface (CPRI), which transmits the digitized in-phase (I) and quadrature (Q) waveforms of the wireless signals, as well as the control words (CWs) used for equipment control and management purpose, in a binary sequence in the time domain [8]. When optical link is used for mobile fronthaul, binary ON–OFF-keying (OOK) is used as the modulation format. One drawback of CPRI is its bandwidth inefficiency due to binary transmission. In the current mobile communication standard of long-term evolution advanced (LTE-A), carrier aggregation (CA) of up to five 20-MHz mobile signals need to be supported. For a system configuration using 8×8 multiple-input and multiple-output (MIMO) and three directional sector antennas (to cover 360° angle geographically), CPRI would require a fronthaul data rate of about 147.5 Gb/s. To support this high fronthaul data rate, a large number of high-speed (e.g., 10 Gb/s) optical OOK transceivers are required.

To achieve bandwidth-efficient mobile fronthaul (EMF), transmission of multiple mobile channels via frequency-division multiplexing (FDM) in a single wavelength channel through analog signal processing that includes frequency conversion and RF combining/splitting has been proposed and numerically studied [9], [10]. Recently, channel aggregation and deaggregation based on digital signal processing (DSP) [11], [12] and analog signal processing [13] have been experimentally demonstrated. Dispersion-penalty-free transmission of six 100-MHz-bandwidth LTE-A-like signals with 36.86-Gb/s CPRI-equivalent data rate over a 40-km standard single-mode fiber (SSMF) fronthaul has been demonstrated by using a single 1550-nm directly-modulated laser (DML) with a modulation bandwidth of only 2 GHz [11]. The dispersion penalty due to the interplay between the fiber chromatic dispersion and the chirp of the DML [14], [15] has been avoided by a novel dispersion-penalty mitigation technique based on judicious mapping of the aggregated signals in the frequency domain. The versatility of the DSP-based channel aggregation approach has been shown in a fronthaul experiment, where 36 evolved universal terrestrial radio access type wireless signals, six for each standardized bandwidth, 1.4, 3, 5, 10, 15, 20 MHz, are aggregated in a single wavelength channel [12]. With the use of a chirp-free Mach–Zehnder modulator, high-throughput channel aggregation of 12 100-MHz LTE-A-like signals has also been demonstrated [13]. This DSP-assisted mobile fronthaul technique has been actively studied within ITU-T Q2/15 regarding Supplement to ITU-T G-series Recommendations related to radio-over-fiber (RoF) technologies and their applications (G Suppl. RoF) [16]–[18].

Manuscript received October 12, 2015; revised December 8, 2015; accepted December 10, 2015. Date of publication December 16, 2015; date of current version March 3, 2016.

The authors are with Futurewei Technologies, Inc., Huawei R&D USA, Bridgewater, NJ 08807 USA (e-mail: xiang.liu@huawei.com; huaiyu.zeng@huawei.com; naresh.chand@huawei.com; frank.effenberger@huawei.com).

Color versions of one or more of the figures in this paper are available online at http://ieeexplore.ieee.org.

Digital Object Identifier 10.1109/JLT.2015.2508451

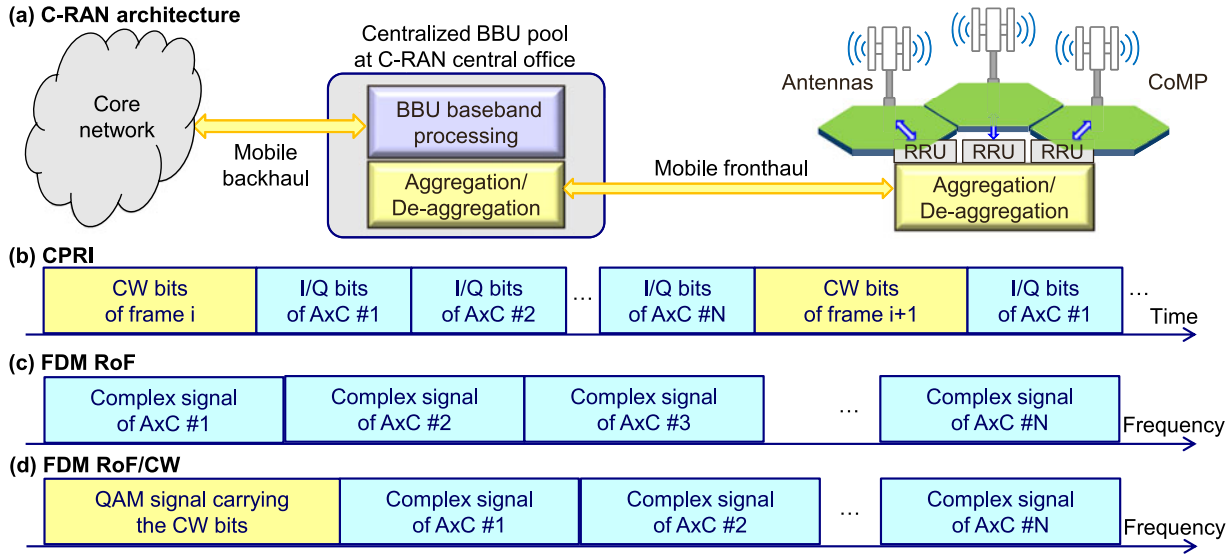

Fig. 1. (a) Schematic of a C-RAN architecture with an optical fiber based mobile fronthaul; (b) TDM of the digitized I/Q bits of antenna-carriers (AxCs) in CPRI; (c) frequency-division aggregation of AxC signals in aggregated RoF; and (d) proposed FDM of AxC signals and a QAM signal that contains the CWs.

To reduce the latency associated with DSP-based channel aggregation and de-aggregation, a novel frequency-domain windowing (FDW) technique to reduce the size of the FFT/IFFT needed for channel aggregation and de-aggregation has been proposed and experimentally demonstrated [19]. Using this FDW technique, a low round-trip DSP latency of <2 μs has been achieved for the aggregation and de-aggregation of 48 20-MHz LTE signals. To make the FDM-based RoF approach [16]–[19] to be compliant with the CPRI interface, the additional transmission of the CWs is needed. Recently, a novel mobile fronthaul transmission scheme has been proposed and demonstrated to achieve bandwidth-efficient transmission of both the I/Q waveforms of wireless signals and the CWs [20]. The CWs are modulated on a single-carrier quadrature amplitude modulation (QAM) signal, which is transmitted synchronously with the wireless signals via FDM. This scheme has been experimentally demonstrated through the transmission of 32 20-MHz LTE signals together with their CPRI-compliant CWs, corresponding to a CPRI-equivalent data rate of 39.32 Gb/s, in single optical channel that requires a RF bandwidth of only $\sim$1.5 GHz [20].

This paper is organized as follows. In Section II, we provide an overview of three mobile fronthaul interfaces, (i) CPRI, (ii) FDM RoF, and (iii) FDM RoF with synchronous transmission of CWs (RoF/CW). In Section III, we describe the DSP implementation of channel aggregation and de-aggregation in FDM RoF and show corresponding experimental results [19]. In Section IV, we present the DSP implementation of FDM RoF/CW and show corresponding experimental results [20]. In Section V, we discuss the feasibility of applying these techniques in future 5G wireless networks to efficiently support both CoMP and M-MIMO. Finally, we provide concluding remarks in Section VI.

II. Mobile Fronthaul Interfaces

Fig. 1(a) shows the schematic of a C-RAN architecture with an optical fiber based fronthaul. For the downlink transmission, the wireless signals generated in a C-RAN central office are aggregated and converted to the optical domain by an optical transmitter. The optical signal is then transmitted through the fiber fronthaul link to reach a remote site, where individual wireless signals intended for different antenna-carriers (AxCs) [8] are de-aggregated and sent to their designated antennas. For the uplink transmission, the reverse of the above operation is applied. For the interface used for fronthaul, it can be based on CPRI, aggregated RoF, and aggregated RoF/CW, as to be discussed in more depth below.

A. CPRI

Fig. 1(b) shows the schematic of the CPRI frame structure, showing the time-domain multiplexing (TDM) of the digitized I/Q bits of multiple AxCs, together with the CWs. Each time-domain sample of a wireless signal is typically digitized to 15 bits for each of the I and Q components of the complex waveform of the signal. The ratio between the bits used for CWs and the I/Q bits is 1:15. Each CRPI basic frame lasts 0.26 μs (1/3.84 MHz), and 256 basic frames form a super-frame. Then 150 super-frames form a 10-ms frame conventionally used in universal mobile telecommunications system. For optical transmission, binary OOK is used. 8b/10b line coding is often used to facilitate OOK clock recovery and error detection. As a typical example, the CPRI data rate needed for aggregating 8 20-MHz LTE signals (with 30.72-MHz sampling rate) in the 8×8 MIMO case is as high as 9.8304 Gb/s ($= 8 \times 2 \times 16 \times 30.72 \times 10/8$ Mbit/s) [8]. This indicates the bandwidth inefficiency of CPRI.

B. FDM RoF

The principle of FDM RoF is to aggregate wireless signals to/from multiple antennas in the frequency domain and to transmit them together over a fiber-based fronthaul link using a single wavelength channel, as shown in Fig. 1(c). The wireless signals aggregated in the optical channel may have their spectral

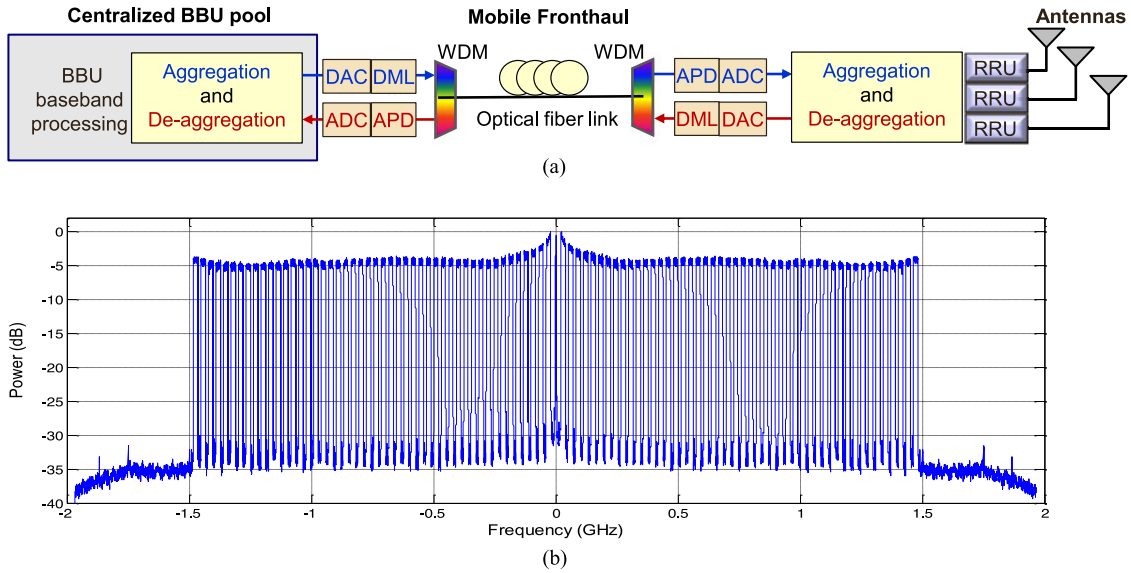

Fig. 2. (a) Schematic of the mobile fronthaul architecture with DSP-based FDM RoF; (b) experimentally measured spectrum of 48 20-MHz LTE signals (and their images due to Hermitian symmetry) that are aggregated using seamless channel mapping and transmitted over 5-km SSMF with –6 dBm received signal power. The signal center wavelength is 1550 nm. DML: directly modulated laser; APD: avalanche photodiode.

bandwidths unchanged, leading to much improved bandwidth efficiency as compared to CPRI. In effect, the transmitted optical signal is an analog signal with a spectral efficiency much higher than the OOK signal used in CPRI. The channel aggregation and de-aggregation can be realized by using efficient DSP based on FFT and IFFT [19].

C. FDM RoF/CW

To facilitate the control and management of the fronthaul equipment and/or to be compliant with CPRI, it is necessary to transmit the CWs alongside the wireless signals. Fig. 1(d) shows the proposed aggregated-RoF/CW scheme where the CWs are modulated by a signal-carrier QAM signal, which is then multiplexed with the wireless signals via FDM [20]. To achieve a bit error ratio (BER) of $<10^{-12}$ for the CWs [8], the constellation size of the QAM signal needs to be chosen based on the signal-to-noise-ratio (SNR) of the fronthaul system. For a typical SNR of ~25 dB, 16-QAM can be used to achieve BER $< 10^{-12}$ with ~1 dB margin. When 16-QAM is used for CW modulation, the spectrum bandwidth needed for CWs is ½ of that needed for the wireless signals. When no CWs are needed to be transmitted, the same optical channel bandwidth can be used to transmit 50% more LTE signals [19].

To reduce the bandwidth needed for transmitting the CWs, higher-level QAM such as 64-QAM may be used, at the expense of higher required SNR. Alternatively, the ratio between the CW bits and the digitized I/Q bits may be reduced from the typical 1:15 ratio specified in CPRI, e.g., to a ratio of 1:63 (or 1:255). This is doable especially for future wireless networks where the wireless signal bandwidth is expected to be much increased while the data rates needed for CWs remain relatively constant. To achieve synchronous transmission of CW bits and I/Q bits, we show that FFT/IFF based block processing can be used, as shown in a following section.

III. EMF With FDM RoF

A. Experimental Setup

Fig. 2(a) shows the schematic of the mobile fronthaul architecture using DSP-based FDM RoF. In LTE-A, MIMO and CA are used. Assuming a representative macro-cell configuration with 8 × 8 MIMO, CA having two 20-MHz mobile signals, and 3 directional sectors, there are totally 48 20-MHz LTE signals. We conduct experiment to investigate the fronthaul performance when these 48 20-MHz LTE signals are aggregated into one single wavelength channel. To achieve high cost-effectiveness, we use intensity-modulation and direct-detection (IM/DD) with a DML and an avalanche photodiode (APD). At the transmitter, we use offline DSP to generate 48 20-MHz LTE OFDM signals. The modulation format is OFDM with 64-QAM subcarrier modulation, which is the highest level modulation specified in LTE. The time-domain waveform of the aggregated signals is stored in an arbitrary waveform generator and outputted by a 3.932-GSa/s digital-to-analog converter (DAC). This analog signal is then amplified before driving a 1550-nm DML with a modulation bandwidth of ~1.5 GHz. The output power from the DML is about 8 dBm. Multiple wavelength channels can be multiplexed by a wavelength-division multiplexer (WDM) to further increase the fronthaul capacity. At the remote location, another WDM can be used to de-multiplex the wavelength channels.

To achieve high-capacity mobile fronthaul with low-bandwidth optics, we use seamless channel mapping. The center frequencies of the signals after aggregation are n × 30.72 MHz, where n = 1, 2, 3, . . . 48. To mitigate the bandwidth-limitation induced power roll-off at high frequencies, a simple digital frequency-domain pre-emphasis is applied at the channel aggregation stage such that $\Delta P(n) = (n–1)/47 \times 4$ dB, where $\Delta P(n)$ is the power change of the n-th signal in dB. The pre-emphasis is based on the system frequency response. For

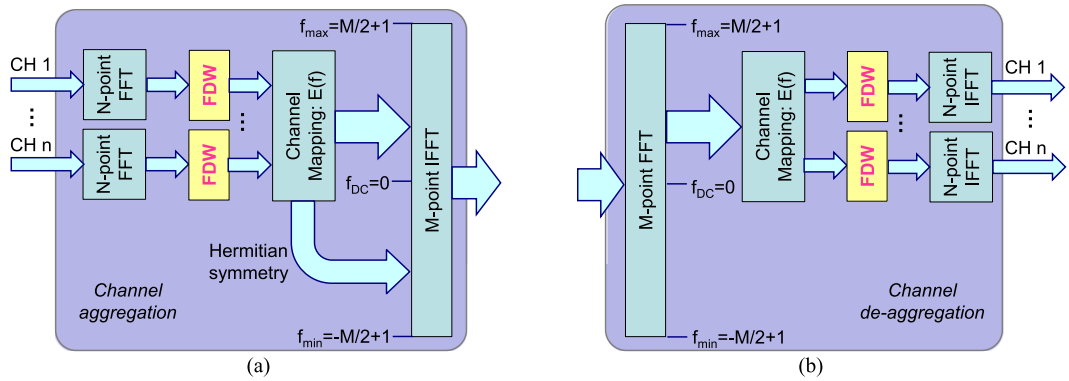

Fig. 3. Schematic of the DSP blocks for FFT/IFFT-based channel aggregation (a) and de-aggregation (b), both with the use of FDW to reduce the DSP processing latency.

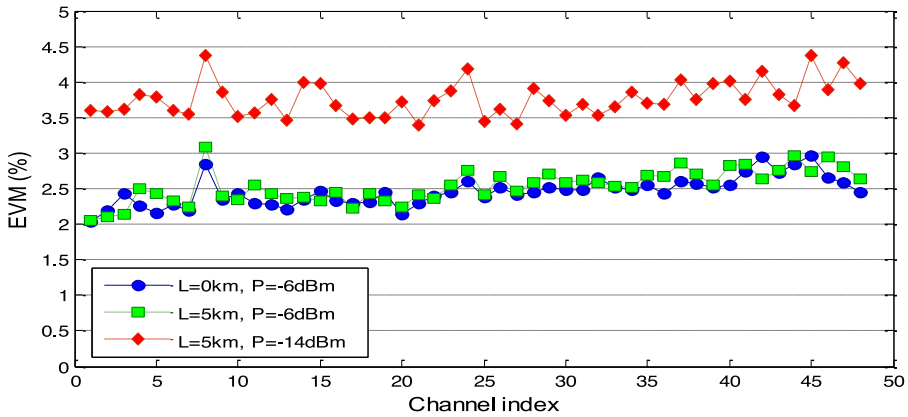

Fig. 4. The EVMs of the 48 LTE signals measured under three conditions, (a) optical back-to-back (L = 0 km) at $P_{RX} = -6$ dBm, (b) after 5-km transmission (L = 5 km) at $P_{RX} = -6$ dBm, and (c) after 5-km transmission (L = 5 km) at $P_{RX} = -14$ dBm.

high-capacity mobile fronthaul applications, the distance between the antennas and the BBUs can be just a few kilometers. We use a 5-km SSMF to emulate the fronthaul link. Note that to avoid fiber dispersion induced penalty for longer fiber links, the wavelength channel can be transmitted in the O-band centered at 1310 nm. After fiber transmission, a variable optical attenuator (VOA) is used to vary the optical power (P_{RX}) received by the APD. The detected signal is digitized by a 10-GSa/s ADC in a real-time sampling scope. The digitized samples are stored in the scope, and later processed by offline DSP for down-sampling, channel de-aggregation, OFDM demodulation, and evaluation of EVM and BER. Fig. 2(b) shows the spectrum of the 48 20-MHz LTE signals measured after the 5-km SSMF transmission at $P_{RX} = -6$ dBm. Clearly, with the use of the digital frequency-domain pre-emphasis, the power spectrum of the received LTE signals is reasonably uniform.

B. Frequency-Domain Windowing

To achieve low latency for FFT/IFFT-based channel aggregation, we add a new FDW process after each N-point FFT, as shown in Fig. 3(a). Similarly, a FDW process is added prior to each N-point IFFT in the channel de-aggregation stage, as shown in Fig. 3(b). The FDW imposes a windowing function that attenuates the high-frequency components and suppresses the inter-channel crosstalk, thereby reducing the FFT/IFFT size and thus the processing latency. With the use of FDW, the N and M values used (in Fig. 3) are reduced by 4 times, to 16 and 2048, respectively. The near-optimum windowing function for the 16-point FFT/IFFT case is found to be [0.44 0.66 0.94 1 1 1 1 1 1 1 1 1 0.94 0.66 0.44] according to [19]. The theoretical overall round-trip DSP-induced latency (including two channel aggregation stages and two de-aggregation stages) is calculated to be ~1.6 μs. With a typical implementation margin of <20%, the practically achievable round-trip DSP latency is estimated to be <2 μs.

C. Experimental Results

To achieve low latency for FFT/IFFT-based channel aggregation, we add a new FDW process after each N-point FFT, as shown Fig. 4 shows the EVMs of all the 48 LTE signals measured under three conditions, (a) optical back-to-back (L = 0 km) at $P_{RX} = -6$ dBm, (b) after 5-km SSMF transmission (L = 5 km) at $P_{RX} = -6$ dBm, and (c) after 5-km SSMF transmission (L = 5 km) at $P_{RX} = -14$ dBm. The first observation is that all the 48 signals have similar EVM values, indicating reasonable performance uniformity in the frequency domain. The second observation is that the signal performances obtained after 5-km SSMF transmission are very similar to those obtained at L = 0 km. This indicates negligible fiber dispersion induced penalty in this scenario. There is a small drop in performance

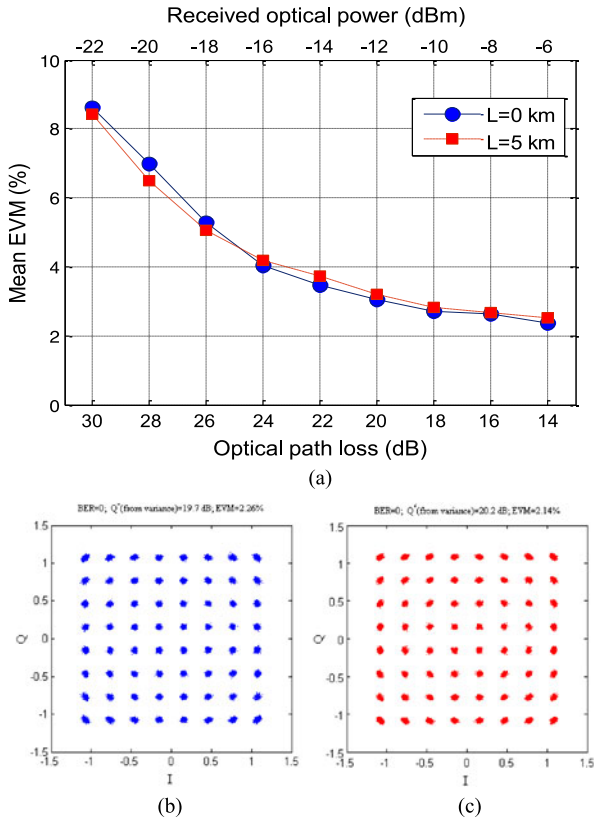

Fig. 5. The mean EVM of the aggregated LTE signals versus optical path loss and received optical power (a) and representative recovered OFDM-64QAM subcarrier constellations for L = 0 km (b) and L = 5 km (c) at $P_{RX} = -6$ dBm.

at the eighth channel, which is attributed to the non-uniform frequency response of the hardware used. Finally, the signal EVMs after 5-km SSMF transmission with $P_{RX} = -14$ dBm are ~2.5%, well below the typical 8% EVM threshold specified for 64-QAM.

Fig. 5 shows the mean EVM of all the signals as a function of the optical path loss and the received optical power, and representative recovered OFDM-64QAM subcarrier constellations for L = 0 km and L = 5 km at $P_{RX} = -6$ dBm. Evidently, there is no noticeable dispersion-induced penalty in this 5-km mobile fronthaul system. At the required EVM threshold of 8% for 64-QAM, the received optical power needs to be larger than −21 dBm. Given the fact that optical signal power generated by the DML-based transmitter is 8 dBm, the optical path loss budget is thus 29 dB, meeting the N1 loss budget requirement for passive optical networks. We expect that with additional performance improvement techniques such as optical pre-amplification, the link loss budget can be further increased.

IV. EMF With FDM RoF/CW

A. DSP Implementation of FDM RoF/CW

Fig. 6 shows the schematic of the DSP-based channel aggregator and de-aggregator for FDM RoF/CW. Without loss of generality, we assume the channel aggregation is for n wireless signals with equal bandwidth as in the case of n×n MIMO. The n digital baseband signals are first converted to the frequency domain by N-point fast Fourier transforms (FFTs). In parallel, the CW bits are modulated via QAM. To facilitate the recovery of the CW bits, training symbols are added in the QAM signal to aid channel synchronization and equalization. The QAM signal is then converted to the frequency domain by a K-point FFT. The values of N and K are chosen based on the bandwidths allocated to the wireless signals and the QAM signal. All the frequency-domain components are mapped onto the input of a single M-point inverse Fourier transform (IFFT). Hermitian symmetry is applied to obtain real-valued output from the IFFT in order to allow the use of low-cost IM/DD for optical transmission. For channel de-aggregation, the reverse of the above is applied, as shown in Fig. 6(b). For the QAM signal, channel estimation and equalization are performed. Finally, the CW bits are recovered by demodulating the equalized QAM signal.

We then verify the DSP implementation through numerical simulation. For channel aggregation, we use 32 20-MHz LTE-like signals, each having a sampling rate of 30.72 MHz, and a 16-QAM signal with a spectral bandwidth of 491.52 MHz. The sizes of the N-FFT, K-FFT, and M-IFFT are 16, 256, and 2048, respectively. The sampling rate of the high-speed DAC and ADC is 3.9322 GSa/s. Additional pulse shaping is performed on the 16-QAM signal. Fig. 7 shows the simulated RF spectrum of the aggregated RoF/CW channel. Evidently, all the signals are aggregated with desired bandwidth and negligible spectral overlap. We will evaluate the transmission performance experimentally in the next section.

B. Experimental Setup and Results

Fig. 8 shows the experimental setup for demonstrating the EMF scheme based on aggregated-RoF/CW. We first generate 32 20-MHz LTE signals with OFDM with 64-QAM subcarrier modulation, and a 491.52-Mbaud 16-QAM signal to carry the CWs. These signals are then aggregated in the frequency domain using the DSP described in the previous section. The time-domain waveform of the aggregated signal is stored in an arbitrary waveform generator and outputted by a 3.9322-GSa/s DAC. This analog signal is then amplified before driving a 1550-nm DML with a modulation bandwidth of about 2 GHz. The generated optical signal has a power of 9 dBm. It is launched into a 5-km SSMF. After fiber transmission, a VOA is used to vary the optical power received by an APD. The detected signal is digitized by a 10-GSa/s ADC in a real-time sampling scope. The digitized samples are stored in the scope, and later processed by offline DSP for down-sampling and channel de-aggregation. The LTE signals are processed by OFDM channel equalization and demodulation, followed by the evaluation of the received signal EVM and BER. The 16-QAM signal is processed by QAM channel equalization and demodulation, followed by the evaluation of the received SNR and BER.

Fig. 9 shows the experimentally measured RF spectrum of the FDM RoF/CW signal after 5-km SSMF transmission at a received optical power of –8 dBm. All the signals are aggregated with desired bandwidth and small spectral overlap. There is a 5-dB drop in signal spectral power density from the low-frequency edge (~0.1 GHz) to the high-frequency edge

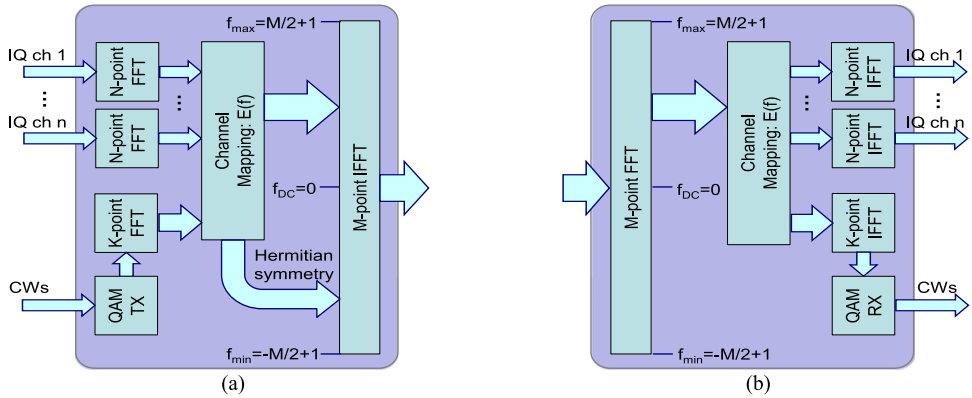

Fig. 6. Schematic of the DSP-based channel aggregator (a) and de-aggregator (b) for aggregated RoF/CW.

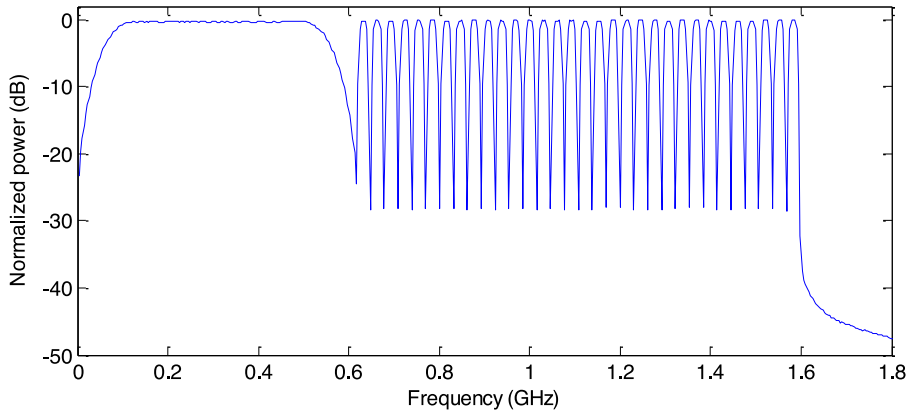

Fig. 7. Numerically simulated RF spectrum of an aggregated RoF/CW channel with 32 20-MHz LTE signals and a CW signal sampled at 491.52 MHz.

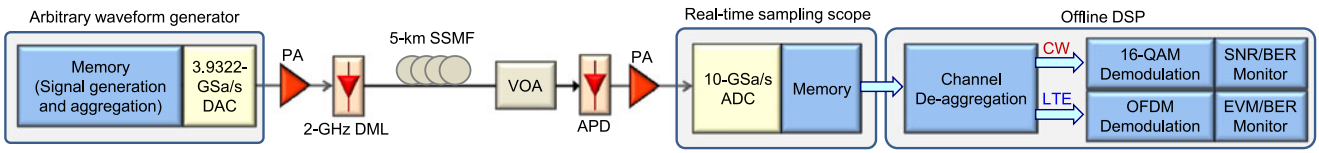

Fig. 8. Experimental setup for evaluating the performance of the proposed aggregated RoF/CW fronthaul transmission scheme.

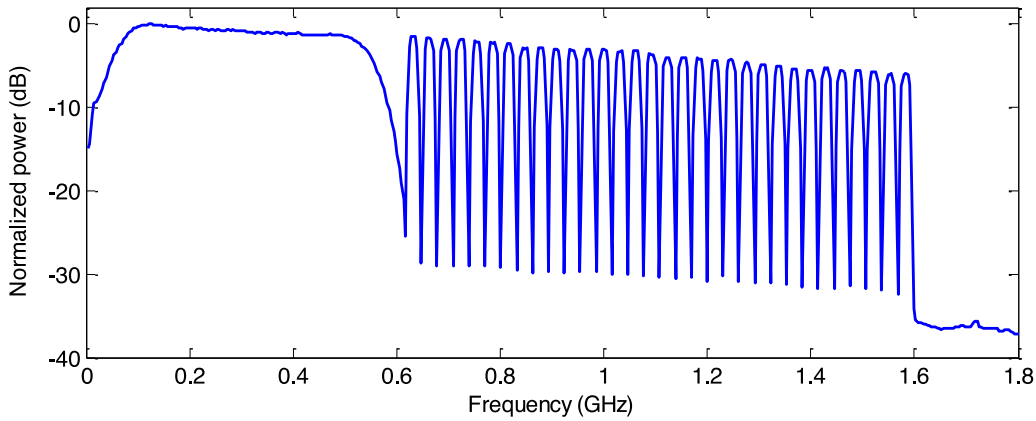

Fig. 9. Experimentally measured RF spectrum of the aggregated-RoF/CW signal after 5-km SSMF transmission at a received optical power of −8 dBm.

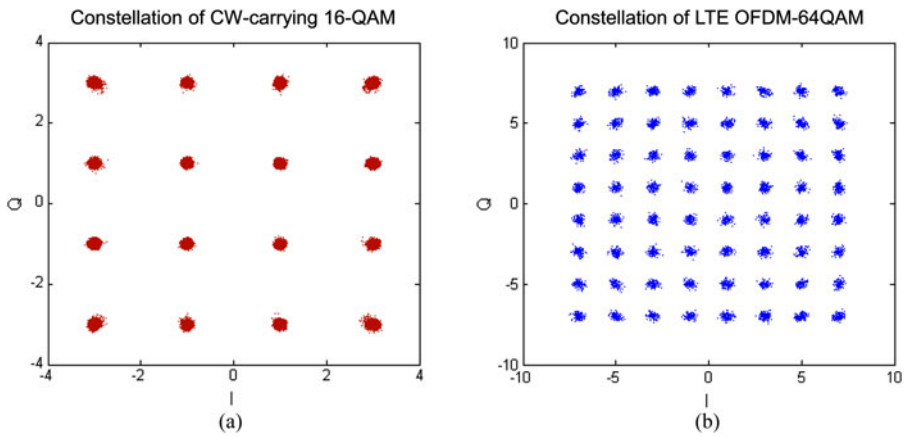

Fig. 10. Experimentally measured constellations of the CW-carrying 16-QAM signal (a) and the LTE OFDM-64QAM signals after 5-km SSMF transmission at a received optical power of −8 dBm.

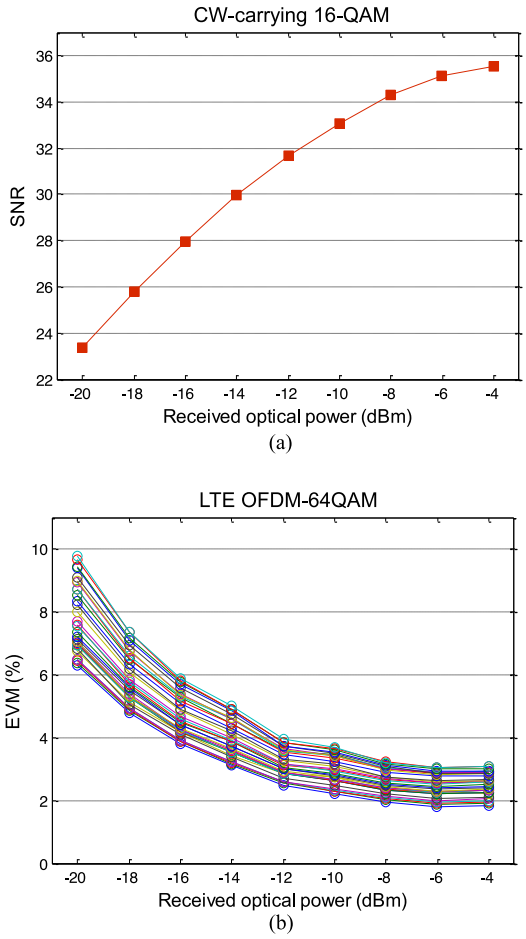

Fig. 11. (a) Experimentally measured SNR versus received optical power for the 491.52-Mbaud CW-carrying 16-QAM signal; (b) experimentally measured EVMs of the 32 20-MHz LTE OFDM-64QAM signals versus received optical power.

(∼1.6 GHz), primarily due to the bandwidth limitation of the DAC and ADC used. The signal spectral power density is 30∼35 dB higher than the noise floor. Fig. 10 shows the experimentally measured constellations of the CW-carrying 16-QAM signal and the LTE OFDM-64QAM signals under the same condition. Evidently, the recovered constellations are of high quality, and no errors are measured with over 10 million bits processed for the LTE signals and the CW carrying 16-QAM signals.

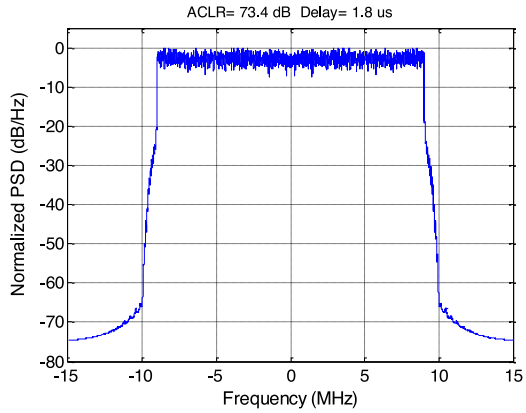

Fig. 12. The RF spectrum of a 20-MHz LTE signal after ACLR suppression by a DSP-based post-filter at the antenna site.

To further quantify the transmission performance of the aggregated-RoF/CW signal, we transmit the signal over 5-km SSMF and vary the optical power received by the APD. Fig. 11(a) shows the received SNR of the CW-carry 16-QAM signal as a function of the received power. The received SNR is measured from the recovered signal constellation, and needs to be over 23 dB to achieve a BER of below 10^{-12}. When the received power is in the range between –20 and –4 dBm, no errors are measured, and the measured SNRs are all above 23 dB. This indicates that CWs can be successfully transmitted over the fronthaul link with 29 dB loss budget.

Fig. 11(b) shows the received EVM of the LTE signals (OFDM-64QAM) versus the received power. The required EVM threshold specified for 64-QAM in LTE-A is 8%. When the received power is higher than −18 dBm, the received EVMs of all the 32 LTE signals are below 8%. With pre-emphasis

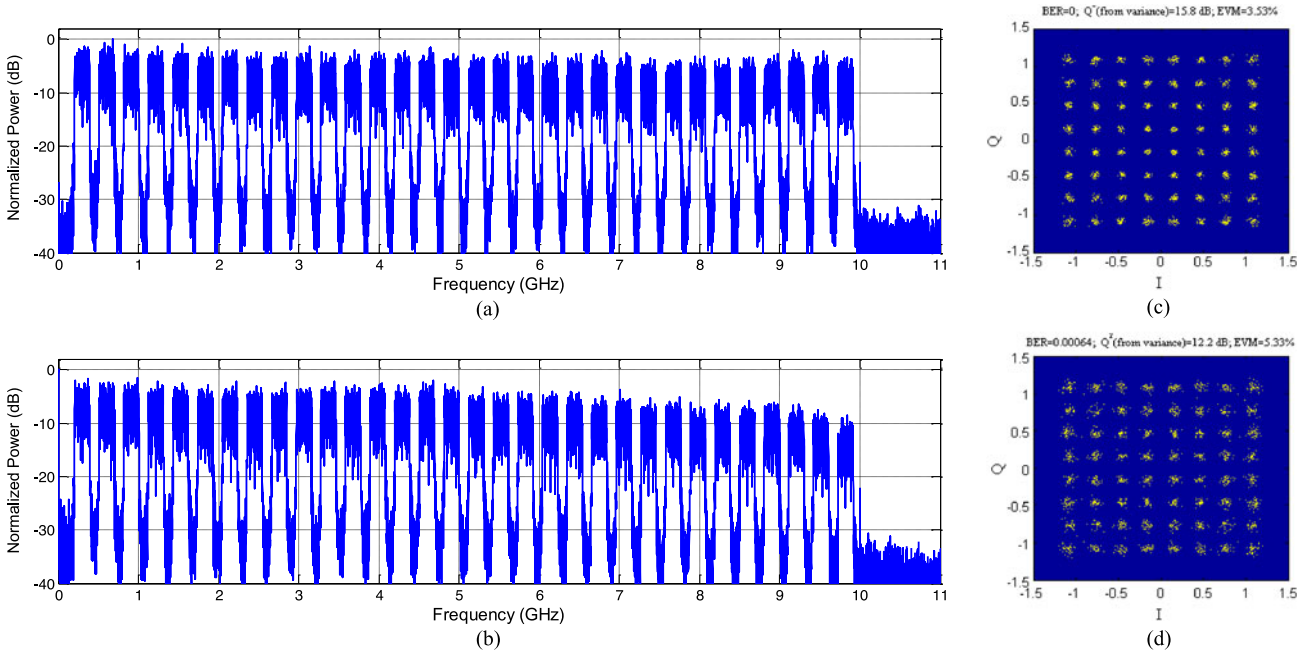

Fig. 13. Experimentally measured RF spectra (a), (b) and constellations (c), (d) of the aggregated 32 200-MHz wireless signals before fiber transmission (a), (c) and after 1-km SSMF transmission in the C-band (b), (d) [22].

to boost the powers of the high-frequency signals, the EVM performances of these 32 LTE signals are expected to become more uniform. When the received power is in the range between −12 and −4 dBm, the received EVMs of all the 32 LTE signals are below 4%. This indicates that the LTE signals can also be successfully transmitted over the fronthaul link with sufficient loss budget in certain passive optical networks (PONs) such as wavelength-division multiplexed PON (WDM-PON) [21].

C. Adjacent Channel Leakage Ratio (ACLR) Reduction via DSP-Based Post-Filtering

It is necessary to reduce the ACLR after fronthaul transmission, in order to avoid inter-channel crosstalk. We show that sufficiently low ACLR can be obtained by DSP-based post-filtering during the channel de-aggregation stage. The post-filter is implemented in the time domain with 72 taps. Fig. 12 shows a 20-MHz LTE signal after post-filtering. The ACLR is suppressed to below −73 dBc. Moreover, the DSPs at the remote sites can also be configured to perform digital pre-distortion to compensate for the nonlinear distortion caused by the power amplifiers before the antennas. This indicates the additional benefits of antenna-site DSP in improving the overall performance of mobile fronthaul.

V. Scaling up Fronthaul Capacity for Future 5G

For future 5G wireless systems, both M-MIMO and large signal bandwidth are expected. For 64 × 64 M-MIMO with 200-MHz signal bandwidth, the CPRI-equivalent data rate per sector would be about 800 Gb/s. For a fronthaul link supporting three such directional sectors, the total data rate required by CPRI would be as high as about 2.4 Tb/s. With the use of the EMF techniques described above and scaling up the modulation and detection speed, it is possible to support 32 200-MHz signals, corresponding to CPRI-equivalent data rate of approximately 400 Gb/s using a single optical wavelength channel. Fig. 13 shows the aggregation of 32 200-MHz wireless signals using 15-GHz-class DML and APD, and 40-GSa/s DAC and ADC. The EVM before and after 1-km SSMF transmission in the C-band are measured to be ∼3.5% and ∼6%, respectively [22]. When operating in the O-band, 20-km transmission distance is expected to be supported.

More recently, a novel CPRI-compatible EMF scheme based on time division multiplexing (TDM) rather than FDM to support the synchronous transmission of CWs and IQ data has been proposed and experimentally demonstrated [23]. 256 Gb/s CPRI-equivalent data rate has been achieved using 10-GHz-class optics. This shows the feasibility of using the EMF approach to bandwidth-efficiently and cost-effectively support future 5G wireless networks.

VI. Conclusion

We have reviewed recent progress on the use of DSP-based FDM RoF for bandwidth-EMF with low latency. More specifically, we have described DSP techniques for channel aggregation and de-aggregation, FDW, ACLR reduction, and synchronous transmission of both the I/Q waveforms of wireless signals and the CWs used for control and management purposes. Relevant experimental results have also been presented. This type of bandwidth-EMF schemes using DSP-based channel aggregation may find applications in supporting C-RAN, CoMP, and M-MIMO in future generations of wireless networks such as 5G.

REFERENCES

[1] China Mobile Research Institute, "C-RAN: The road towards green RAN," Whitepaper v. 2.6, Sep. 2013.

[2] Z. Shen, A. Papasakellariou, J. Montojo, D. Gerstenberger, and F. Xu, "Overview of 3GPP LTE- advanced carrier aggregation for 4G wireless communications," *IEEE Commun. Mag.*, vol. 50, no. 2, pp. 122–130, Feb. 2012.

[3] K. Werner, H. Asplund, B. Halvarsson, N. Jalden, and D. Figueiredo, "LTE-A field measurements: 8 × 8 MIMO and carrier aggregation," presented at the IEEE Vehicular Technology Conf., Dresden, Germany, 2013.

[4] A. Pizzinat, P. Chanclou, T. Diallo, and F. Saliou, "Things you should know about fronthaul," presented at the Eur. Conf. Optical Communication, Cannes, France, 2014, Paper Tu.4.2.1.

[5] Y. Okumura and J. Terada, "Optical network technologies and architectures for backhaul/fronthaul of future radio access supporting big mobile data," presented at the Optical Fiber Communication Conf., San Francisco, C A, USA, 2014, Paper Tu3F.1.

[6] N. Cvijetic, A. Tanaka, K. Kanonakis, and T. Wang, "SDN-controlled topology-reconfigurable optical mobile fronthaul architecture for bidirectional CoMP and low latency inter-cell D2D in the 5G mobile era," *Opt. Exp.*, vol. 22, no. 17, pp. 20809–20815, 2014.

[7] E. Larsson, O. Edfors, F. Tufvesson, and T. Marzetta, "Massive MIMO for next generation wireless systems," *IEEE Commun. Mag.*, vol. 52, no. 2, pp. 186–195, Feb. 2014.

[8] CPRI Specification V6.1, "Common public radio interface (CPRI): Interface specification," Jul. 2014.

[9] D. Wake, A. Nkansah, and N. J. Gomes, "Radio over fiber link design for next generation wireless systems," *IEEE/OSA J. Lightw. Technol.*, vol. 28, no. 16, pp. 2456–2464, Aug. 2010.

[10] S.-H. Cho *et al.*, "Cost-effective next generation mobile fronthaul architecture with multi-IF carrier transmission scheme," presented at the Optical Fiber Communication Conf., San Francisco, CA, USA, 2014, Paper Tu2B.6.

[11] X. Liu, F. Effenberger, N. Chand, L. Zhou, and H. Lin, "Efficient mobile fronthaul transmission of multiple LTE-A signals with 36.86-Gb/s CPRI-equivalent data rate using a directly-modulated laser and fiber dispersion mitigation," presented at the Asia Communications Photonics Conf., Shanghai China, 2014, Paper AF4B.5.

[12] X. Liu, F. Effenberger, N. Chand, L. Zhou, and H. Lin, "Demonstration of bandwidth-efficient mobile fronthaul enabling seamless aggregation of 36 E-UTRA-like wireless signals in a single 1.1-GHz wavelength channel," presented at the Optical Fiber Communication Conf., Los Angeles, CA, USA, 2015, Paper M2J.2.

[13] M. Zhu, X. Liu, N. Chand, F. Effenberger, and G.-K. Chang, "High-capacity mobile fronthaul supporting LTE-advanced carrier aggregation and 8 × 8 MIMO," presented at the *Optical Fiber Communication Conf.*, 2015, Paper M2J.3.

[14] C.-C. Wei, "Small-signal analysis of OOFDM signal transmission with DML and direct detection," *Opt. Lett.*, vol. 36, no. 2, pp. 151–153, 2011.

[15] N. S. Andr´e, H. Louchet, K. Habel, and A. Richter, "Analytical formulation for SNR prediction in DMDD OFDM-based access systems," *IEEE Photon. Technol. Lett.*, vol. 26, no. 12, pp. 1255–1258, Jun. 15, 2014.

[16] T. Kuri, Ed. *Supplement ITU-T G-Series Recommendations Related Radio-Over-Fiber Technologies Their Applications*, 2015.

[17] Futurewei Technologies, Inc., "Aggregated analog radio over fiber (AA-ROF)," ITU-T SG15 Plenary Meet. COM15-C0889, Nov. 2014.

[18] ETRI, SK Telecom, "Multiple radio signal downlink transmission based on IF-band RoF transmission scheme," ITU-T SG15 Plenary Meet. COM15-C1048, Nov. 2014.

[19] X. Liu, H. Zeng, N. Chand, and F. Effenberger, "Experimental demonstration of high-throughput low-latency mobile fronthaul supporting 48 20-MHz LTE signals with 59-Gb/s CPRI-equivalent rate and 2-μs processing latency," presented at the Eur. Conf. Optical Communication, Valencia, Spain, 2015, Paper We.4.4.3.

[20] X. Liu, H. Zeng, and F. Effenberger, "Bandwidth-efficient synchronous transmission of I/Q waveforms and control words via frequency-division multiplexing for mobile fronthaul," presented at the *GLOBECOM*, San Diego, CA, USA, 2015, Paper SAC 21-3.

[21] D. Nesset, "NG-PON2 technology and standards," presented at the Eur. Conf. Optical Communication, Cannes, France, 2014, Paper Mo.4.1.1.

[22] X. Liu, H. Zeng, N. Chand, and F. Effenberger, "Bandwidth-efficient mobile fronthaul transmission for future 5G wireless networks," presented at the Asia Communications Photonics Conf., Hong Kong, 2015, Paper ASu3E.4.

[23] X. Liu, H. Zeng, N. Chand, and F. Effenberger, "CPRI-compatible efficient mobile fronthaul transmission via equalized TDMA achieving 256 Gb/s CPRI-equivalent data rate in a single 10-GHz-bandwidth IM-DD Channel," in *Proc. Opt. Fiber Commun. Conf.*, 2016, Paper W1H.3.

Xiang Liu (M'00–SM'05) received the Ph.D. degree in applied physics from Cornell University, Ithaca, NY, USA, in 2000. He is currently the Director of the Optical Access Networks Department of Futurewei Technologies, Huawei R&D USA, Bridgewater, NJ, USA, focusing on next-generation optical access technologies. He had been a Distinguished Member of Technical Staff at Bell Labs New Jersey, working on high-speed optical fiber communication. He has authored/coauthored more than 300 journal and conference papers, and holds more than 60 U.S. patents. He is a Fellow of the OSA and an Associated Editor of the *Optics Express*. He has also served as a Technical Program Committee Chair for several international optical communication conferences such as OFC, ACP, and WOCC.

Huaiyu Zeng received the Ph.D. degree in electrical engineering from the University of Connecticut, Storrs, CT, USA, in 1997. He was with Lucent/Philips Consumer Communications, AT&T Labs-Research, Intel Corporation, and Broadcom Corporation. His focus was primarily on physical layer and audio signal processing for mobile handset development, smart antenna prototype system, DSL physical layer development, etc. Since 2015, he has been working with Optical Access Networks Department at Futurewei Technologies, Huawei R&D USA, Bridgewater, NJ, USA. His research interests include digital signal processing technologies in digital communication systems and audio signal processing. He holds more than 40 U.S. patents.

Naresh Chand received the M.Sc. degree in microwave engineering from the Birla Institute of Technology and Science, Pilani, India, and the Ph.D. degree in electrical engineering from the University of Sheffield, Sheffield, U.K., in 1983. He is currently with the Optical Access Networks Department of Futurewei Technologies, Huawei R&D USA, Bridgewater, NJ, USA. Prior to this, he was an Engineering and Technology Fellow with BAE Systems, Wayne, NJ. Prior to joining BAE Systems in 2003, he was a Distinguished Member of Technical Staff with Agere Systems where he conducted research in optical communications and networks. From 1986 through 2000, he was with AT&T/Lucent Bell Laboratories on optical access, communication lasers, and high-speed electronics technologies. During 1974–1979, he was with the Government of India where he was involved in development of electronics industry in India.

Frank Effenberger (F'15) received the Doctoral degree in 1995. He was with Bellcore (now Telcordia) where he analyzed all types of access network technologies, focusing on those that employed passive optical networks. He witnessed the early development of the FSAN initiative and the APON standard. In 2000, he moved to Quantum Bridge Communications, where he managed the system engineering group. This work supported the development and standardization of advanced optical access systems based on B-PON and G-PON technologies. In 2006, he became the Director of FTTx in the Advanced Technology Department of Futurewei Technologies USA, Bridgewater, NJ, USA. He remains heavily involved in standards work, and in 2008, he became the Chairman of ITU-T Q2/15. He and his team work on forward-looking fiber and copper access technologies, including the 10G EPON, XG-PON, and 40G-PON. Notably, his team supported the world's first trials of XG-PON and 40G-PON. In 2011, he was named as Huawei Fellow, and in 2012 was promoted to VP of access research. In 2015, he was named as a Fellow of the OSA. He holds more than 60 U.S. patents.